What is Responsible for the Strong Observed Asymmetry in Teleconnections Between El Niño and La Niña?

Tao Zhang[1,2], Judith Perlwitz[1,2], and Martin P. Hoerling[2]

[1]Cooperative Institute for Research in Environmental Sciences

University of Colorado

Boulder, Colorado

[2]NOAA Earth System Research Laboratory

Physical Sciences Division

Boulder, Colorado

(*Submitted to Geophysical Research Letters*)

Accepted on January 20, 2014

Corresponding author address:

Dr. Tao Zhang

NOAA/ESRL/PSD

325 Broadway, R/PSD1

Boulder, CO 80305

Email: tao.zhang@noaa.gov

Abstract

A large asymmetric component (El Niño+La Niña) of ENSO-related teleconnections over North America is found during 1984-2009 that is comparable in strength to the commonly studied symmetric component (El Niño – La Niña). Climate reforecasts spanning this period are diagnosed in order to understand the processes responsible for the observed asymmetry. It is confirmed that an asymmetric component is indeed a fundamental property of atmospheric responses to recent ENSO forcing. Each and every composite of a 16-member reforecast ensemble has appreciable asymmetry in tropical Pacific rainfall, upper tropospheric Pacific-North American circulation patterns, and contiguous U.S. surface temperatures. There is considerable sampling variability in the magnitude of this asymmetric component among individual reforecast composites. We argue therefore that the true SST boundary forced signal of ENSO teleconnections is likely comprised of a symmetric component having greater magnitude than its asymmetric component, though the latter is an important property of how ENSO affects North American climate.

1. Introduction

Neither the tropical Pacific oceanic expression nor the accompanying atmospheric teleconnections of El Niño–Southern Oscillation (ENSO) are mirror images of each other [e.g. *Hoerling et al.* 1997, 2001; *Monahan and Dai* 2004; *Wu et al.* 2005; *Hannachi et al.* 2003; *An and Jin* 2004; *Zhang et al.* 2011]. Given that ENSO is the primary source of U.S. seasonal forecast skill [e.g. *Quan et al.* 2006], it is of predictive value to better understand these higher-order characteristics. It is likewise important to assess sophisticated dynamical forecast systems, and evaluate their ability to reproduce the observed cold and warm event impact patterns and not just linear regression modes of such impacts [e.g. *Larkin and Harrison* 2002].

Observational composites of the wintertime U.S. surface temperature anomalies for ENSO events since the early 1980s reveal the asymmetric anomalies (El Niño+La Niña) to be of comparable magnitude to the symmetric anomalies (El Niño-La Niña) (see Figure 1). Here we explore the factors responsible for such strong asymmetry. Energy balance studies have revealed the physical processes undergirding the symmetric and asymmetric components of observed North American ENSO-related surface temperature anomalies [*Zhang et al.* 2011]. Likewise, process studies have argued that the observed North American surface asymmetric component of ENSO impacts are physically reconcilable with asymmetries in atmospheric circulation anomalies [e.g. *Wu et al.* 2005]. The fundamental question of what is responsible for the large magnitude of observed asymmetry in teleconnections between El Niño and La Niña remains open, however.

The current study utilizes a new historical reforecast data set of dynamical seasonal predictions for the period 1984-2009 generated by the National Center's for

61 Environmental Prediction (NCEP) Climate Forecast System (CFS) version 2 [*Saha et al.*
62 2013]. Using initialized short lead predictions, and applying resampling strategies that
63 take advantage of the large ensembles, we derive statistical distributions of symmetric
64 and asymmetric components of teleconnection patterns. These permit a separation of the
65 contributions by true SST forcing from contributions by random sampling variability, and
66 thus clarify the causes for the recent ENSO teleconnection characteristics.
67
68 **2. Data and Methods**
69 CFSv2 produces a set of 9-month retrospective forecasts with the model
70 initialized using observations from the CFS reanalysis [*Saha et al.* 2010]. In this study,
71 we employ the sixteen-member CFSv2 reforecasts with one-month lead-time of
72 individual northern winter months December, January, February from which seasonal
73 means (DJF) are determined (see auxiliary material for specific dates of initial conditions
74 used for the sixteen-member reforecasts). *Kim et al.* [2012] showed that CFSv2 captures
75 the main ENSO teleconnection pattern of stronger anomalies over the tropics, the North
76 Pacific and the North America, and predicts the interannual variation associated with
77 ENSO quite accurately.
78 This study focuses on the recent period 1984-2009 for which reforecasts are available.
79 Following the study of *Zhang et al.* [2011], we construct anomaly composites relative to
80 the reference period 1984-2000 and based on six El Niño (1986/87; 1987/88; 1991/92;
81 1994/95; 1997/98; 2002/03) winters and five La Niña (1988/89; 1995/96; 1998/99;
82 1999/2000; 2007/08) winters.

The symmetric component of the ENSO signal is determined as the difference between El Niño (warm) and La Niña (cold) anomaly composites while the asymmetric component is defined as the sum of El Niño and La Niña anomaly composites [*Hoerling et al.* 1997]. The root mean square (RMS) of the asymmetric component over the region of concern is used as a metric to quantify the strength of the asymmetry. A large sample of composites is obtained based on the sixteen members of warm and cold composites from the reforecasts by looping over independent warm and cold events drawn from different model realizations. This approach allows to generate a total of 256 asymmetry estimates (see auxiliary material for details).

For comparison with reforecasts, the following observational data sets are used: 500 hPa geopotential height fields from the National Centers for Environmental Prediction (NCEP)–National Center for Atmospheric Research (NCAR) reanalysis [*Kalnay et al.* 1996], observed land surface temperature from the gridded land-based Climatic Research Unit (CRU) temperature database (CRUTEM4) [*Jones et al.* 2012], SST data from the Hadley Centre Sea Ice and SST (HadISST) dataset [*Rayner et al.* 2003], precipitation from the Climate Prediction Center (CPC) Merged Analysis of Precipitation [*CMAP; Xie and Arkin* 1997].

3. Results

Figure 1 displays the wintertime observed asymmetric (left panel) and symmetric (right panel) components of ENSO composites for 500 hPa heights (top), North American surface temperature (second row), tropical Pacific SSTs (third row), and tropical Pacific rainfall (bottom). Consistent with the findings of *Hoerling et al.* [1997]

106 which were based on a mostly earlier collection of ENSO cases, the composite of cases
107 during only the last quarter century also exhibits prominent asymmetry in circulation
108 anomalies over the Pacific-North American region. The symmetric component of 500
109 hPa height anomalies over the North Pacific is much stronger than the asymmetric
110 component. Over North America, each has similar magnitude and both describe high
111 pressure over central Canada. As a consequence of this latter similarity in magnitudes,
112 the strength of North American surface temperature anomalies is likewise quite similar
113 for symmetric and asymmetric composites, with each having a maximum southern
114 Canada/northern U.S. warming. The two temperature patterns are nonetheless readily
115 distinguishable from each other, with the symmetric component having a dipole structure
116 whereas the asymmetric component describes a monopole continent-wide warming. In
117 this sense, the asymmetric component appears not to be a residual of the symmetric
118 ENSO signal that might occur, for instance, if the El Niño anomalies were merely
119 stronger than the La Niña anomalies.

120 The asymmetries in the wintertime North Pacific-North American expressions of
121 ENSO impacts instead arise primarily from a phase shift between the El Niño and La
122 Niña patterns. In particular, the former has anticyclonic anomalies over central Canada
123 that reside 25° longitude east of the latter's cyclonic anomaly (see Figure S1 in the
124 auxiliary material). This asymmetry in upper level height composites is the underlying
125 cause for the large asymmetry in North American surface temperatures as discussed in
126 detail in *Zhang et al.* [2011] and argued previously by *Wu et al.* [2005].

127 There are several mechanisms that may be responsible for this strong observed
128 asymmetry in teleconnections between El Niño and La Niña over North America. One is

129 that the tropical forcing itself is asymmetrical with respect to ENSO's extreme opposite
130 phases, as originally argued in *Hoerling et al.* [1997]. The lower panels of Figure 1
131 indeed reveal that the El Niño and La Niña SST composites are not symmetric. There is a
132 spatial phase shift in the SST anomalies themselves, with warming (cooling) during El
133 Niño (La Niña) being greater in the eastern (western) equatorial Pacific (see Figure S1).
134 Likewise, equatorial Pacific rainfall anomalies, which constitute the immediate forcing
135 for the atmospheric teleconnections themselves, are not symmetric (Figure 1, bottom). In
136 this sense, the asymmetric component of *extratropical* teleconnections could be
137 reconciled with a multi-linearity of atmospheric circulation responses (i.e. different
138 teleconnections are each linearly related to different patterns of ENSO forcing) which are
139 phase shifted owing to displacements in their SST and atmospheric convective forcings.
140 Another factor may involve inherent nonlinearity in the atmosphere itself, as
141 demonstrated in idealized atmospheric model simulations of *Lin and Derome* [2004] who
142 argued that asymmetry in teleconnection responses can result from the large
143 modifications in the basic state.

144 A further factor, addressed herein, is sampling variability. First, we verify that the
145 CFSv2 reforecasts are suitable tools, and show that the ensemble mean ENSO composites
146 for events during 1984-2009 for 500 hPa teleconnections, surface temperature responses,
147 and patterns of tropical forcing compare favorably with observational counterparts (see
148 Figure S2). Next, we diagnose the asymmetric (left panels) and symmetric (right panels)
149 responses of the ensemble mean reforecasts (Figure 2). The symmetric component is
150 remarkably similar to its observational counterpart, while the modeled asymmetric
151 component is much weaker than observed, primarily in the extratropics (see Figure 1).

Over the North Pacific and North American regions, the weaker asymmetry in this ensemble of model reforecasts is principally due to a reduced phase shift between El Niño and La Niña 500 hPa teleconnections compared to that observed (see Figure, S2).

Yet, the asymmetry in the model's tropical forcing, including its predicted SSTs and rainfall, are as large as those observed (cf. Figures 1 and 2). Therefore, an appreciable component of the strong observed asymmetry in teleconnections between El Niño and La Niña may be entirely unrelated to forcing. To address the sampling variability in ENSO composites, the individual reforecasts for 1984-2009 are resampled yielding a 256 sample size of composites. We have verified that each of these samples has virtually identical composite SSTs, and thus the variability in atmospheric composites among them stems from random variability. Figure 3 displays the scatter of root mean square (RMS) values in asymmetric components of Pacific-North American 500 hPa heights versus asymmetric components in U.S. surface temperatures for the individual reforecast composites. All samples have asymmetry, indicating that asymmetry is a fundamental property of atmospheric responses to recent ENSO forcing. There is nonetheless considerable spread among the samples, with RMS values of the asymmetry in surface temperature ranging from 0.5^{o}C to 2.3^{o}C, while that of the 500 hPa heights ranges from 10m to 32m. Furthermore, there is a positive correlation (0.61) between the RMS values of 500 hPa heights and surface temperature indicating that the asymmetry in the circulation over the PNA region significantly drives asymmetry in North American surface temperatures.

The observed asymmetric values (red square in Figure 3) reside within the distribution of model samples, with many reforecast composites having weaker

asymmetry and some having stronger asymmetry. To illustrate the spatial pattern of climate anomalies for the extremes in this reforecast distribution, Figure 4 shows the asymmetric component of 500 hPa height and North American surface temperature based on an average of extreme weak and strong asymmetry samples (blue and red closed circles in Figure 3, respectively). It is clear that the strong asymmetry subset (right panels) is in closer agreement to observations (see Figure 1) than the weak asymmetry subset (left panels). The comparison between these two subsets further demonstrates that the stronger asymmetry in 500 hPa circulation drives a stronger asymmetry in North American surface temperature, consistent with a positive correlation noted earlier (Figure 3). Finally, we note that while there are substantial differences in the asymmetric component of extratropical climate impacts among these model subsets, differences in asymmetric components of their tropical Pacific SST forcing (as well as global SSTs) are negligible (not shown). Indicated hereby is the large internal variability in asymmetry of ENSO's extratropical teleconnections.

4. Summary and discussion

The present study provides modeling evidence that an asymmetric component of wintertime ENSO teleconnections (El Nino+La Nina) over North America is a fundamental feature of recent events. In particular, analysis of reforecast experiments indicates that substantial portions of the central U.S. and eastern U.S. experience warm winters during both El Niño and La Niña events, and that the asymmetric component of North American temperatures overall is generally a warming pattern. The large magnitude of the recent observed North American temperature asymmetry during ENSO is not due to forcing alone, however, as indicated by the considerable sampling variability

found among ensemble members of the reforecasts. The observed composites of 6 El Niño and 5 La Niña events are thus not pure indications of the asymmetric component of forced signals associated ENSO extreme phases, and atmospheric noise unrelated to boundary forcing can, and likely has, exerted appreciable influence.

Reforecast experiments further reveal that asymmetry in mid-tropospheric circulation is the key driver for asymmetry in North American surface temperature patterns during ENSO, with stronger circulation asymmetry driving stronger surface temperature asymmetry as previously argued from empirical studies [e.g. *Hoerling et al.* 1997; *Wu et al.* 2005; *Zhang et al.* 2011]. The correlation between the two variables is about 0.6, suggesting that other mechanisms besides the upper tropospheric teleconnection asymmetry may also contribute to ENSO related North American surface temperature asymmetry. For instance, ENSO-related U.S. surface energy calculations reveal an important wintertime effect of snow cover [e.g. *Zhang et al.* 2011], anomalies of which can sometimes arise from a single storm and thus be uncorrelated with seasonal mean 500 hPa heights.

We do not expect that climate variations on decadal and longer time scales significantly affect the present results due to the following reasons. First, the anomalies are computed relative to the climatology over the recent period of reference. Second, observational estimates of ENSO asymmetry in North American surface temperature over several previous periods (1879-1908; 1909-1950; 1951-1983) are within the sampling variability determined from the CFSv2 reforecast ensemble over the 1984-2009 period (not shown).

The physics of the effect of SST forcing on teleconnection asymmetry is not addressed in this study. Future research will attempt to determine whether the teleconnection asymmetry is owing to some fundamental nonlinearity in the atmospheric response to warm versus cold states of the tropical Pacific, or owing to a multi-linearity in atmospheric responses to SST forcings that are somewhat different during El Niño and La Niña. It is evident, however, that as a consequence of the fundamental nonlinearity in ENSO's extratropical impacts, multi-decadal warm (or cold) periods could arise solely from fluctuations in ENSO variance, with enhanced variance (such as has occurred in the last several decades) contributing to a residual warming of North America. Quantifying this effect, and comparing to the signal of anthropogenic forcing, will require additional study.

Acknowledgments

The support offered by the NOAA Climate Program Office Modeling, Analysis, Predictions and Projections (MAPP) Program under grant GC11-300 is gratefully acknowledged. We thank two anonymous reviewers for their helpful comments.

References

An, S-I., and F-F. Jin (2004), Nonlinearity and asymmetry of ENSO, *J. Clim.,*, **17,** 2399–2412.

Hannachi, A., D. Stephenson, and K. Sperber (2003), Probability-based methods for quantifying nonlinearity in the ENSO, *Climate Dyn*, **20,** 241–256.

Hoerling M. P., A. Kumar, and M. Zhong (1997), El Niño, La Niña, and the nonlinearity of their teleconnections, *J. Clim.*, 10, 1769–1786.

Hoerling, M., A. Kumar, and T. Xu (2001), Robustness of the nonlinear climate response to ENSO's extreme phases, *J. Clim.*, **14,** 1277–1293.

Jones, P.D., Lister, D.H., Osborn, T.J., Harpham, C., Salmon, M. and C.P. Morice (2012), Hemispheric and large-scale land surface air temperature variations: an extensive revision and an update to 2010, *J. Geophys. Res.*, doi:10.1029/2011JD017139.

Kalnay, E., et al. (1996), The NCEP/NCAR 40-year reanalysis project, *Bull. Am. Meteorol. Soc*., 77, 437–471.

Kim H.-M., P. J. Webster, and J. A. Curry (2012), Seasonal prediction skill of ECMWF System 4 and NCEP CFSv2 retrospective forecast for the Northern Hemisphere Winter, *Clim. Dyn*., 39, 2957-2973, doi:10.1007/s00382-012-1364-6.

Larkin, Narasimhan K., and D. E. Harrison (2002), ENSO Warm (El Niño) and Cold (La Niña) Event Life Cycles: Ocean Surface Anomaly Patterns, Their Symmetries, Asymmetries, and Implications, *J. Clim.*, **15**, 1118–1140.

Lin, H., and J. Derome (2004), Nonlinearity of the Extratropical Response to Tropical Forcing, *J. Clim.*, **17**, 2597–2608.

268 Monahan, A. H., and A. Dai (2004), The Spatial and Temporal Structure of ENSO
269 Nonlinearity, *J. Clim.*, **17**, 3026–3036.
270 Quan, X., M. P. Hoerling, J. Whitaker, G. Bates, and T. Xu (2006), Diagnosing sources
271 of U.S. seasonal forecast skill, *J. Clim.*, **19**, 3279–3293.
272 Rayner, N. A., D. E. Parker, E. B. Horton, C. K. Folland, L. V. Alexander, D. P. Rowell,
273 E. C. Kent, and A. Kaplan (2003), Global analyses of sea surface temperature, sea ice
274 and night marine air temperature since the late nineteenth century, *J. Geophys. Res.*,
275 **108,** 4407. doi:10.1029/2002JD002670.
276 Saha, S., and Coauthors (2010), The NCEP climate forecast system reanalysis, *Bull.*
277 *Amer. Meteor. Soc.*, **91**, 1015–1057.
278 Saha, S., et al. (2013), The NCEP Climate Forecast System Version 2, *J. Clim.,* doi:
279 http://dx.doi.org/10.1175/JCLI-D-12-00823.1 (in press).
280 Wu, A., W. W. Hsieh, and A. Shabbar (2005), The Nonlinear Patterns of North American
281 Winter Temperature and Precipitation Associated with ENSO, *J. Clim.*, **18**, 1736–
282 1752.
283 Xie P. P, and P. A Arkin (1997), Global precipitation: A 17-year monthly analysis based
284 on gauge observations, satellite estimates, and numerical model outputs, *Bull. Amer.*
285 *Meteor. Soc.*, 78, 2539–2558.
286 Zhang, T., M. P. Hoerling, J. Perlwitz, D.-Z. Sun, and D. Murray (2011), Physics of U.S.
287 surface temperature response to ENSO, *J. Clim.*, **24**, 4874–4887.
288

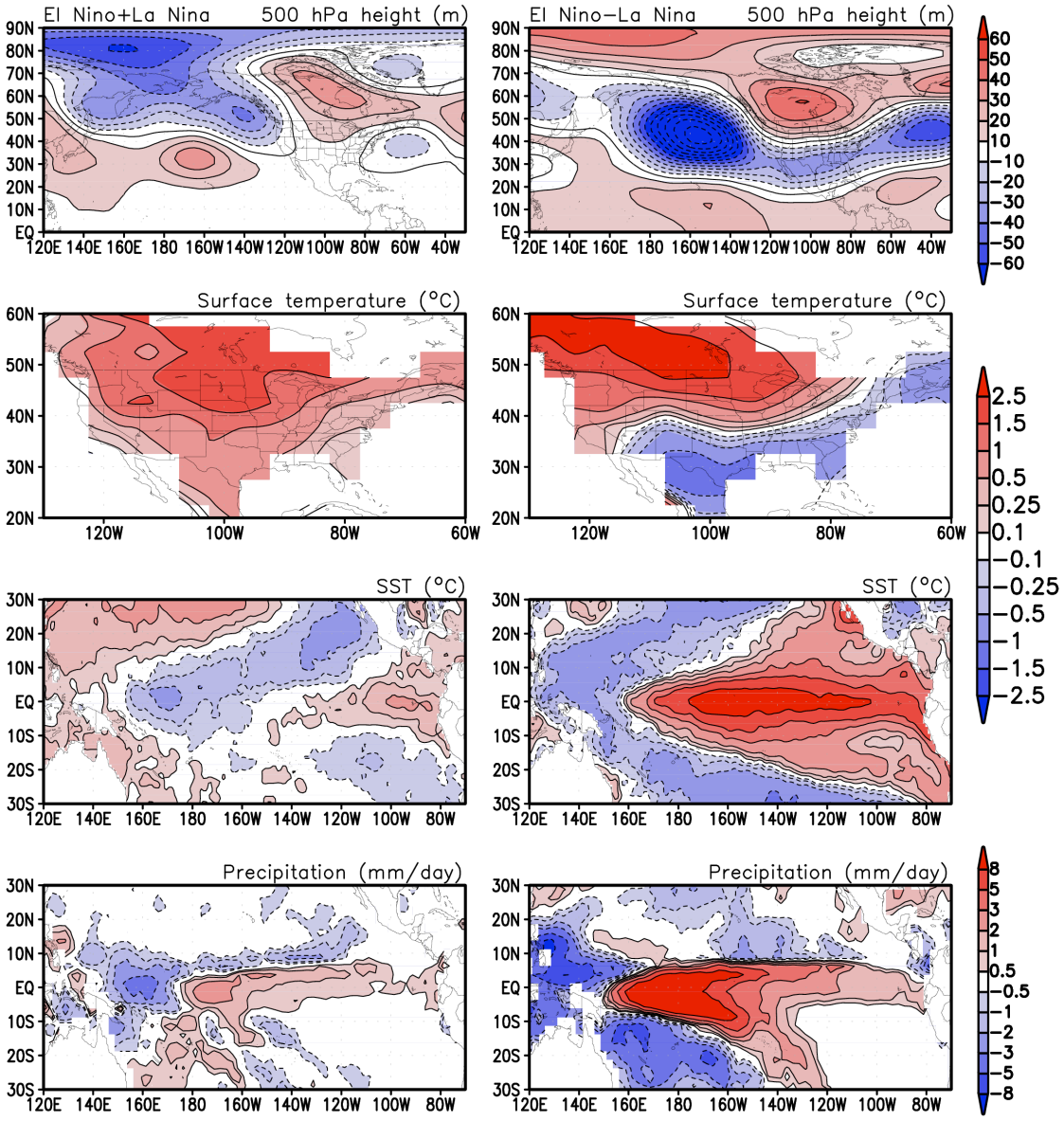

Figure 1: The observed asymmetric (left panel) and symmetric (right panel) components of the ENSO responses for the composite anomalies of wintertime (DJF) 500 hPa geopotential height, land surface temperature, tropical SST and precipitation. See section 2 for the years included in the composites.

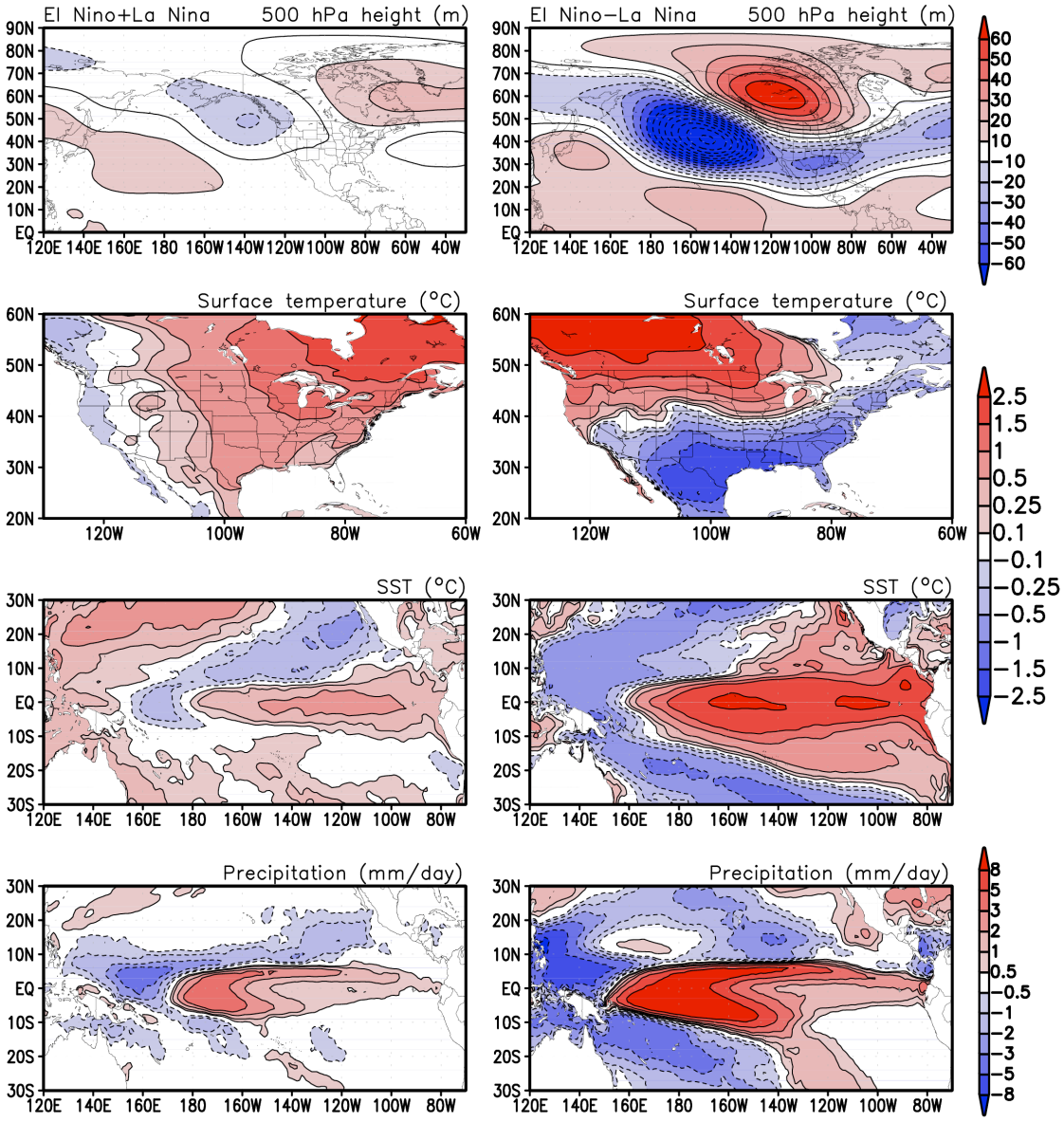

Figure 2: As in Figure 1, but for the CFSv2 reforecasts. Shown are the ensemble mean results from 256 members of the CFSv2 reforecasts.

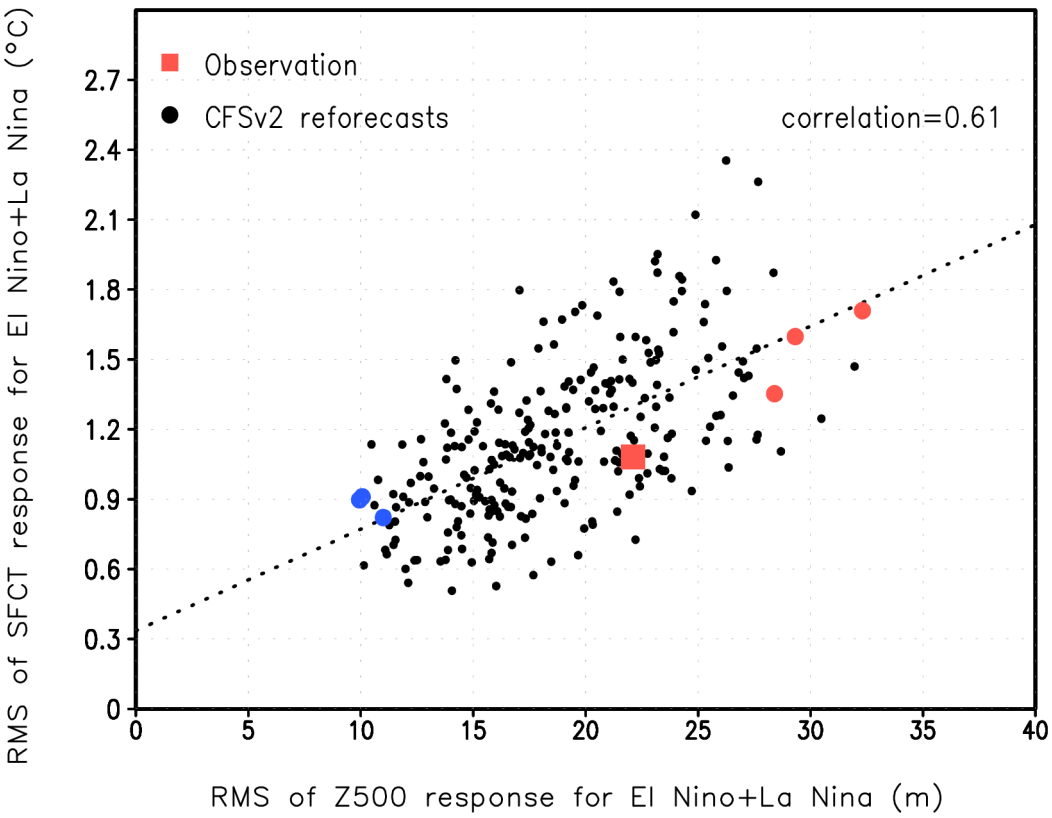

Figure 3: The relationship between the root mean square (RMS) of the asymmetry in DJF 500 hPa height over the Pacific-North America region (120°E-60°W, 30°N-75°N) and the root mean square of the asymmetry in DJF land surface temperature over the North America (130°W-60°W, 20°N-60°N). The closed circles correspond to 256 members of the CFSv2 reforecasts, and the red (blue) closed circles indicate the members that have the top (bottom) three RMS values of the asymmetry in DJF 500 hPa height and are obtained by independent warm and cold events. The observational values are indicated by the red square. Inset value is for the correlation based on 256-member CFSv2 reforecasts.

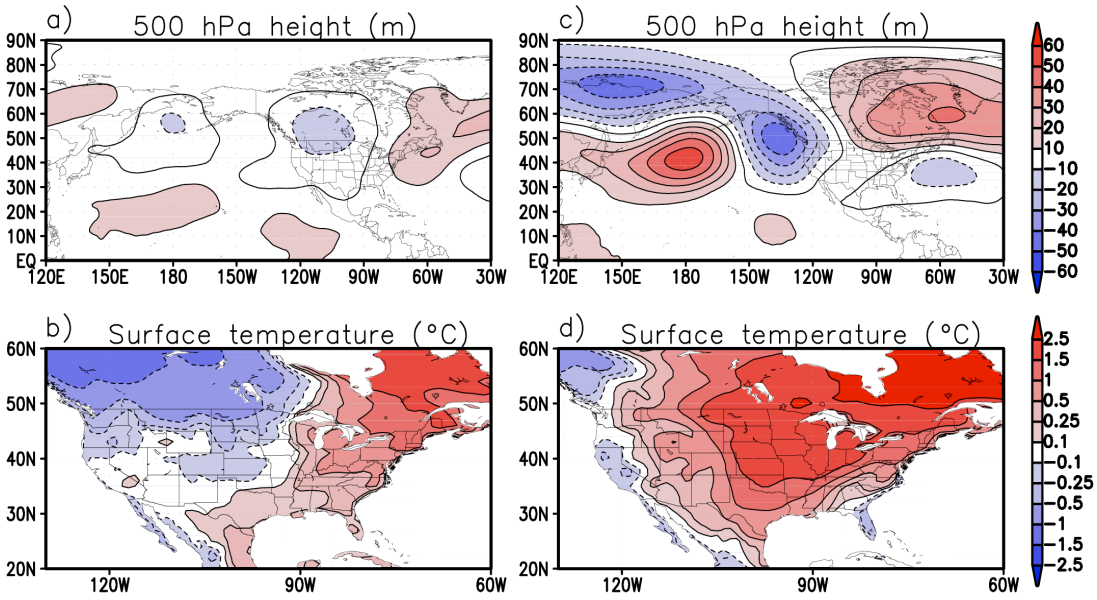

Figure 4: The spatial pattern of the asymmetry in (a) 500 hPa height and (b) land surface temperature from the ensemble mean of three members with small RMS values of the asymmetry in DJF 500 hPa height (indicated by blue closed circles in Figure 3). The corresponding results for the ensemble mean of three members with large RMS values (indicated by red closed circles in Figure 3) are shown in the right panel (c~d) respectively.

The auxiliary material for

What is Responsible for the Strong Observed Asymmetry in Teleconnections Between El Niño and La Niña?

Tao Zhang, Judith Perlwitz, and Martin P. Hoerling

1) *The specific dates of initial conditions used for the sixteen-member CFSv2 reforecasts:* We use the sixteen-member CFSv2 reforecasts with one-month lead-time of individual northern winter months December, January, February for the period 1984-2009. In detail the sixteen-member December reforecasts are taken from the model runs initialized four times daily (00Z, 06Z, 12Z, 18Z) on the following four days: November 12, November 17, November 22, and November 27. The sixteen-member January reforecasts are taken from the model runs initialized four times daily (00Z, 06Z, 12Z, 18Z) on the following four days: December 12, December 17, December 22, and December 27. The sixteen-member February reforecasts are taken from the model runs initialized four times daily (00Z, 06Z, 12Z, 18Z) on the following four days: January 11, January 16, January 21, and January 26.

2) Details for the generation of the 256 asymmetry estimates:

There are sixteen runs (R1 to R16) available for the period from 1984 to 2009. From each run a cold (C1 to C16) and warm (W1 to W16) ENSO composite is determined using the six El Niño (1986/87; 1987/88; 1991/92; 1994/95; 1997/98; 2002/03) winters for the warm composite and the five La Niña (1988/89; 1995/96; 1998/99; 1999/2000; 2007/08) winters for the cold composite, respectively. An asymmetry estimate is calculated as the sum of a warm and cold composite (W+C). For each of the sixteen independent warm composites (W1 to W16), sixteen asymmetry composites can be calculated by utilizing the sixteen cold composites as follows: W1+C1,...,W1+C16,…,W16+C1,…,W16+C16) This approach provides a total number of 256 (16x16) asymmetry estimates.

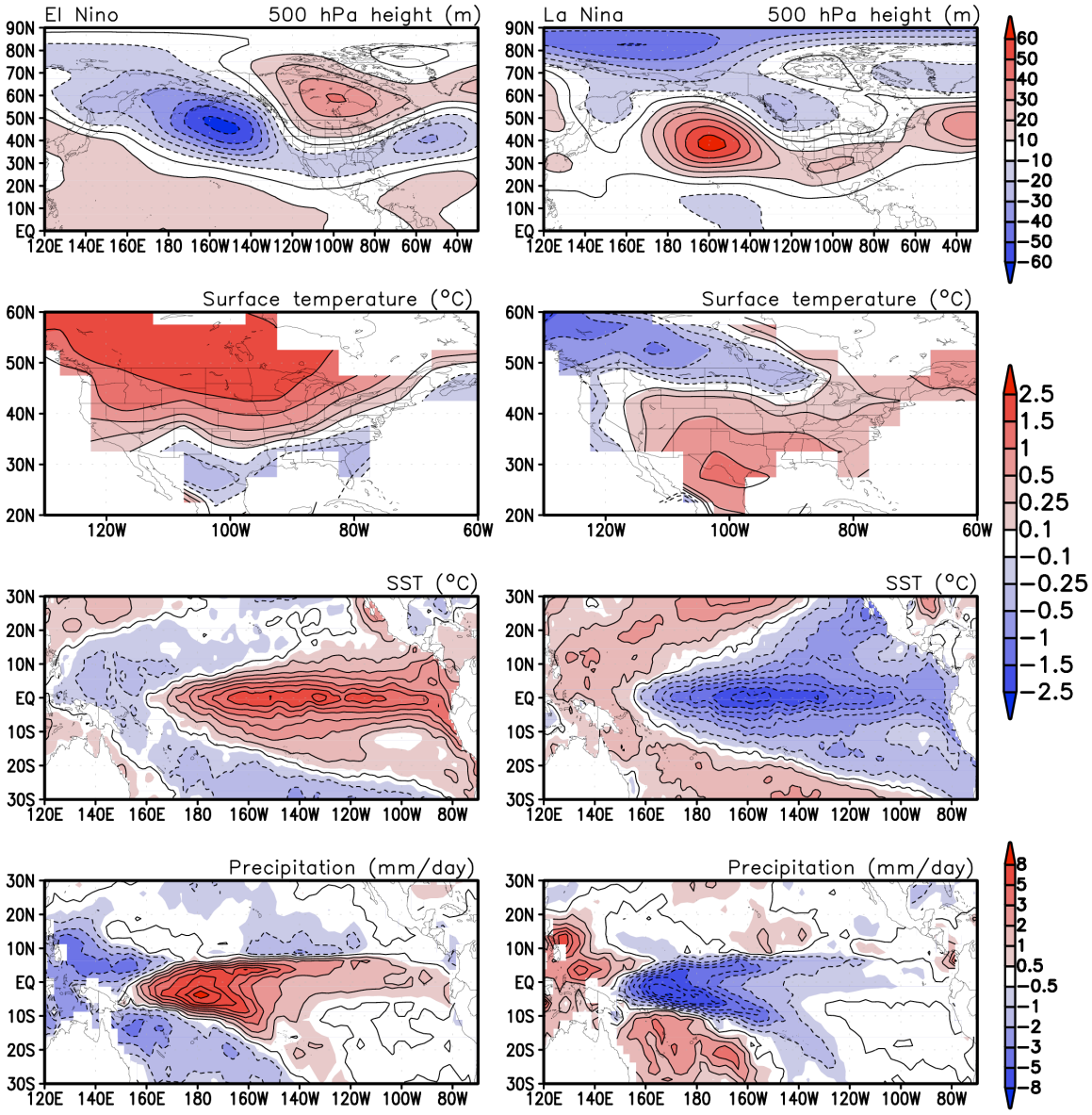

Figure S1: The observed composite anomalies during the warm phase (left panel) and cold phase (right panel) of ENSO for wintertime (DJF) 500 hPa geopotential height, land surface temperature, tropical SST and precipitation.

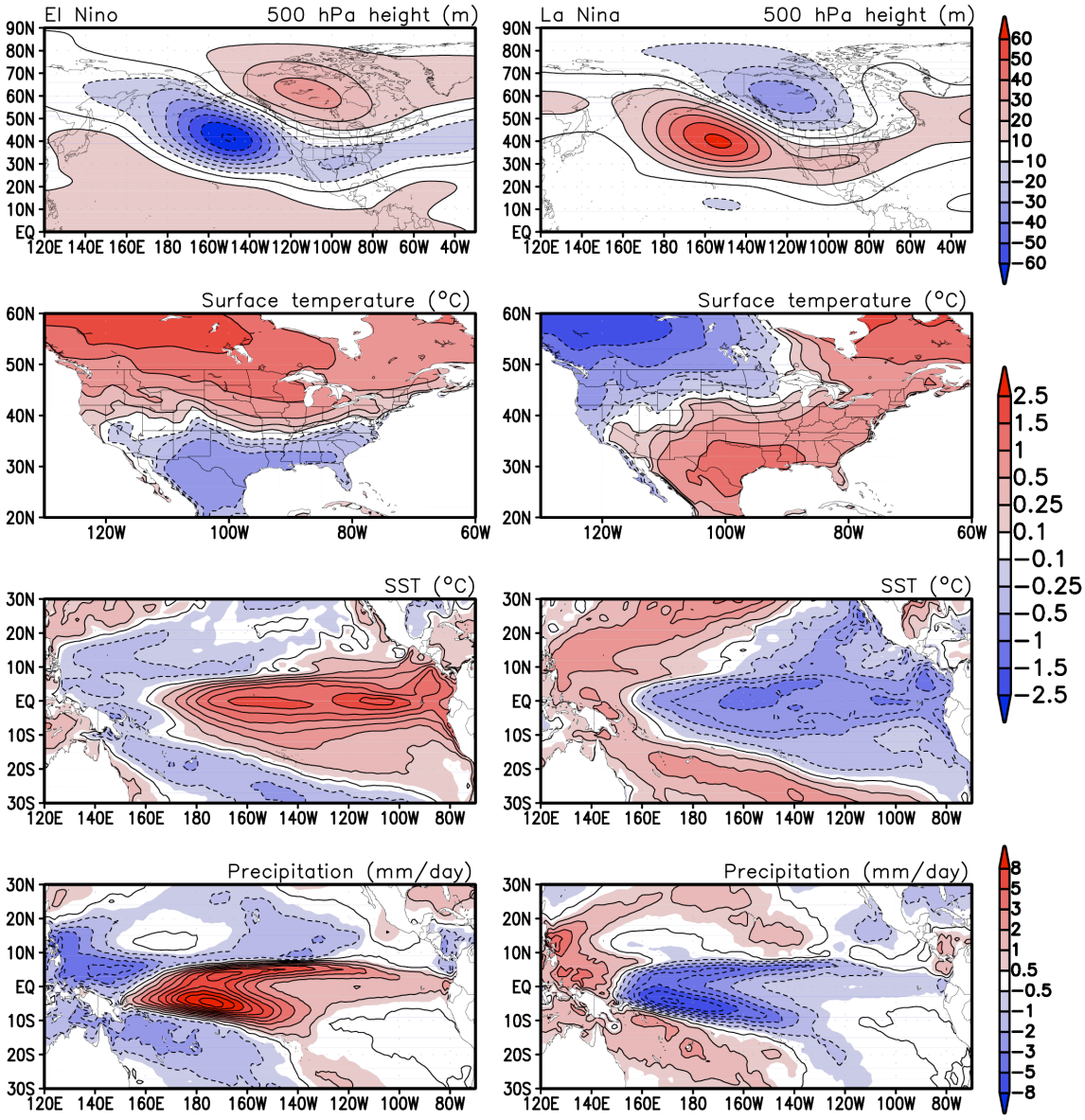

Figure S2: As in Figure S1, but for the CFSv2 reforecasts. Shown are the ensemble mean results from 256 members of the CFSv2 reforecasts.